LARGE-SCALE BIOLOGY ARTICLE

The RootChip: An Integrated Microfluidic Chip for Plant Science [W][OA]

Guido Grossmann,[a] Woei-Jiun Guo,[a,1] David W. Ehrhardt,[a] Wolf B. Frommer,[a] Rene V. Sit,[b,c] Stephen R. Quake,[b,c] and Matthias Meier[b,c,2,3]

[a] Department of Plant Biology, Carnegie Institution for Science, Stanford, California 94305
[b] Howard Hughes Medical Institute, Stanford, California 94605
[c] Departments of Applied Physics and Bioengineering, Stanford University, Stanford, California 94305

Studying development and physiology of growing roots is challenging due to limitations regarding cellular and subcellular analysis under controlled environmental conditions. We describe a microfluidic chip platform, called RootChip, that integrates live-cell imaging of growth and metabolism of *Arabidopsis thaliana* roots with rapid modulation of environmental conditions. The RootChip has separate chambers for individual regulation of the microenvironment of multiple roots from multiple seedlings in parallel. We demonstrate the utility of The RootChip by monitoring time-resolved growth and cytosolic sugar levels at subcellular resolution in plants by a genetically encoded fluorescence sensor for glucose and galactose. The RootChip can be modified for use with roots from other plant species by adapting the chamber geometry and facilitates the systematic analysis of root growth and metabolism from multiple seedlings, paving the way for large-scale phenotyping of root metabolism and signaling.

INTRODUCTION

Roots act as the interface between plants and soil. They take up water and nutrients; respond to changing environmental conditions, such as water availability, nutrient concentration, pH, and salinity; and secrete exudates. To understand the molecular basis of acclimation processes within living root tissue, technical advances are needed to perform assays at cellular resolution while varying the root environment. Important performance parameters include the speed and reproducibility with which environmental changes can be made, ease of reversibility, stability of environmental conditions over time, and the ability to perform assays in multiplex to improve experimental efficiency. Perfusion chambers (Chaudhuri et al., 2011) offer flexibility and high performance in changing environment conditions but, classically, are used one root at a time. In addition, roots are particularly sensitive to physical damage and dehydration, for example, when mounting them in chambers for observation.

Multiplexing in 96-well plates has proven useful in chemical screens of seedling roots (Bassel et al., 2008), and gellan gum–based systems have been developed for mutant screens of root growth and morphology (Clark et al., 2011). However, it is challenging to make precise and rapid environmental changes in these formats and to obtain images at cellular resolution with ease. Hence, there is demand for perfusion systems that can be applied to study cellular processes at high resolution, without specimen handling and in multiplex.

Microfluidics, which refers to the study and control of fluidic properties and their content in structures of micrometer dimensions (Whitesides, 2006), provides powerful platforms to interrogate whole organisms. In single-celled organisms that are otherwise difficult to trap under perfusion conditions, the employment of microfluidic devices has greatly advanced analyses of physiological processes and thus has allowed measurement of ion and metabolite levels in individual yeast cells (Bermejo et al., 2011). For multicellular model organisms, such as the animals *Drosophila melanogaster* (Lucchetta et al., 2005) and *Caenorhabditis elegans* (Gilleland et al., 2010), microfluidic chips have been developed for high-throughput sorting, transferring, stimulating, and/or specific cell manipulating of the organisms. The technical innovation microfluidics offers for these model animals has facilitated high-throughput studies on the organismic level by decreasing costs and experimental times and concomitantly increasing the accuracy of the experiments (Chung et al., 2011; Samara et al., 2010).

However, for plants, this technical advance has not been accomplished yet. A study with *Arabidopsis thaliana* roots on a microfluidic chip has been demonstrated but on a low integration level (Meier et al., 2010).

We describe a microfluidic device, called the RootChip, to integrate parallel root culturing with temporal and content controlled perfusion for roots on a live imaging platform. The utility of RootChip is demonstrated with *Arabidopsis* roots expressing a genetically encoded fluorescence sensor for Glc and Gal based on Förster resonance energy transfer (FRET) measurements. Such FRET sensors allow for noninvasive real-time detection of metabolite levels and fluxes in living tissues (Okumoto, 2010). Subcellular resolution can be achieved by targeting the sensors with specific signaling sequences to different cellular compartments.

RESULTS AND DISCUSSION

Design and Use with *Arabidopsis*

The RootChip is fabricated from polydimethylsiloxane (PDMS) and uses integrated micromechanical push-up valves to guide fluid flow (Unger et al., 2000). The flow layer contains a bifurcating tree element to address eight individual observation chambers (Figures 1A and 1C). The biocompatibility of *Arabidopsis* roots with PDMS has been demonstrated previously (Meier et al., 2010). The nominal channel width and height of the bifurcating tree element is $100 \times 20 \ \mu m$, and the root observation channel is $800 \times 100 \ \mu m$, respectively. Access to the root chambers is provided by holes running from the top of the chip into the observation and perfusion chamber.

Arabidopsis seeds were germinated under controlled temperature and light conditions (90 to 120 $\mu E \ m^{-2} \ min^{-1}$; 16-h-day/8-h-night cycle) in conical cylinders produced from micropipette tips that are filled with agar ($\sim$4 μL volume) and inserted into sterile agar plates. During the first 5 d, the roots grew gravitropically into the plastic cone. After 5 d, the tips including seedlings ($\sim$5 mm total length) were plugged into the access holes of The RootChip (Figures 1B and 2A).

Germination can be achieved in mounted plastic tips filled with solid medium on the chip for full integration. Germination outside the chip platform allows for preselection of seedlings by screening for desired properties, such as adequate root length, to avoid lack of germination or poor growth or seedling health or to avoid insufficient expression of a fluorescence sensor. Moreover, external growth also allows for defined pretreatments (e.g., drug incubation). Humidity is controlled by a custom-made chip carrier, which contains water reservoirs and by the ability to cover the chip by a transparent lid (Figures 2A to 2C).

Roots grow from the solid agar medium in the pipette tips into the observation chamber of the PDMS device (Figure 2A), which was prefilled with liquid medium. All of these manipulations should be performed under sterile conditions. Growth is monitored regularly by bright-field microscopy; once the root tip enters the observation chamber, the setup is connected to a pressure line with a computer-controlled actuated valve system and transferred to a suitable inverted microscope for wide-field fluorescence or confocal observation. The device can be mounted vertically or horizontally. Since vertical mounting of a microscopic specimen requires specialized microscopes, we demonstrate its use here only with the widely used inverted setup.
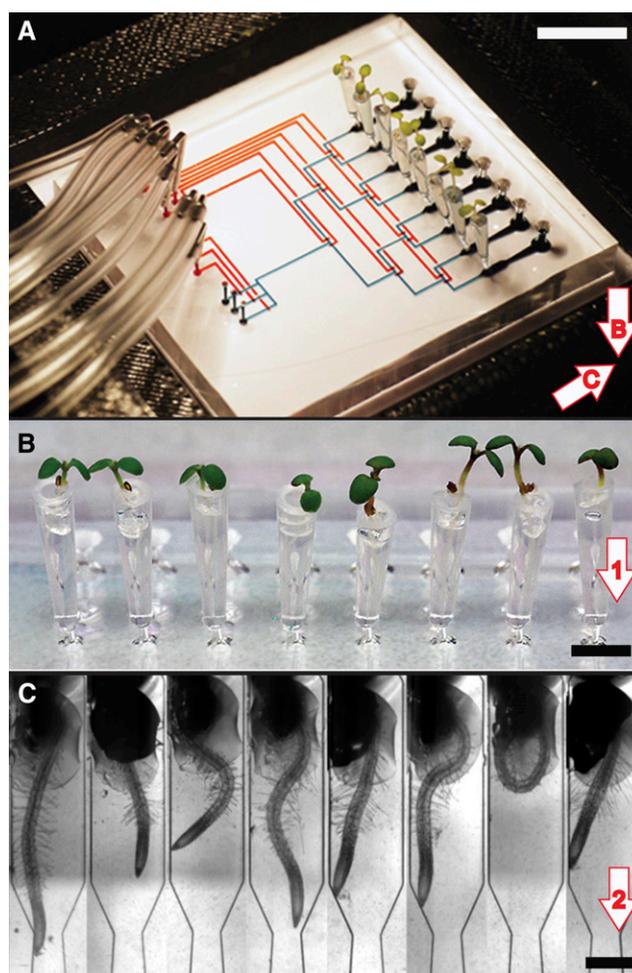

Figure 1. The RootChip.

(A) Image of a PDMS chip with eight mounted live plants. Control and flow channels of the chip are filled for illustration with red and blue food coloring, respectively. Bar = 1 cm.

(B) Top view of the eight plants in conical cylinders filled with agar and mounted onto the chip. Arrow indicates the growth direction of the root. Bar = 0.5 cm

(C) Bottom view of the microchannels containing roots of seedlings 7 d after germination (cf. Supplemental Movies online). Arrows indicate the perspective for **(B)** and **(C)**. Bar = 0.5 mm.

Perfusion of the root is initiated using hydroponic medium at low flow pressure (1 to 2 p.s.i.). The vertical part of the root chamber connected to the tip has a length of $\sim$100 μm; thus, once reaching the bottom of the microfluidic channel, the root changes its growth orientation from a vertical to a horizontal direction, typically aligning with the flow direction (Figure 2A). To facilitate growth toward the outlet, inlet holes for root entry are punched with a tilt of 30°. On average, seven out of eight roots grew in the direction of the outlet and were useful for perfusion experiments. Leakage through the entry hole is avoided by manufacturing the outlet diameter 3 times larger than the entry hole, resulting in an $\sim$50-fold lower flow resistance for the outlet.
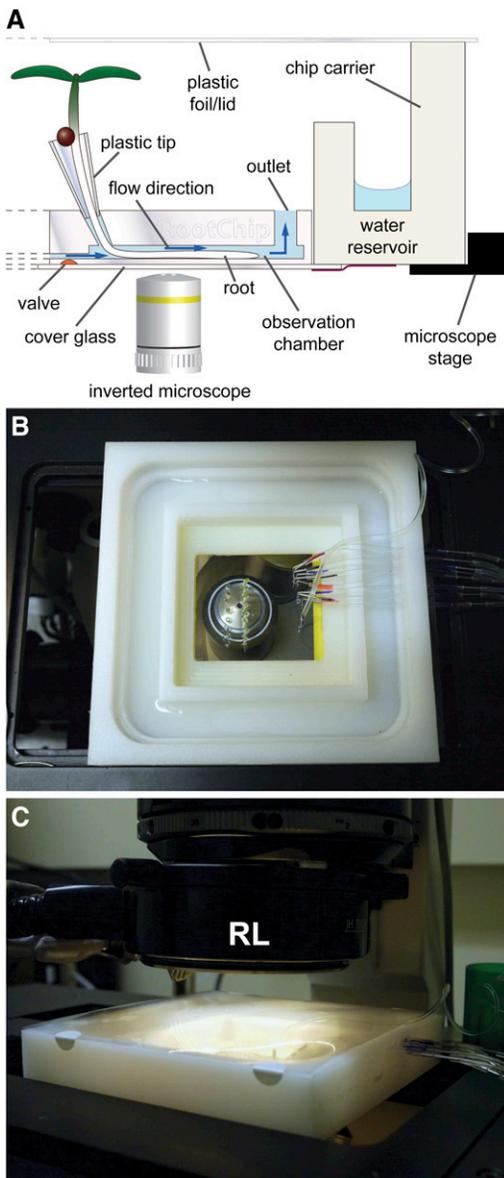
Figure 2. Mounting and Use of The RootChip.

(A) Scheme (not to scale) of RootChip being mounted on a microscope stage using the chip carrier.
(B) Top view of The RootChip and carrier on the stage under experimental conditions with the plastic foil removed.
(C) During plant growth on the microscope, the device is covered to maintain high humidity and illuminated with a ring light (RL).

Arabidopsis roots have been shown to respond to horizontal growth on agar plates with elevated ethylene production, which causes reduction in growth rate (Okamoto et al., 2008). Notably, we observed no difference in root growth in this setup compared with growth on vertical plates; the average growth rate on plates during days 6 to 8 after germination was 2.6 ± 0.1 μm min^{-1}, whereas average growth rate over 24 h on the RootChip was 2.6 ± 0.2 μm min^{-1}. A possible explanation could be that the constant flow of media prevents accumulation of secreted metabolites or hormones.

Monitoring Cytosolic Glc and Gal

The RootChip was used to monitor cytosolic Glc and Gal levels in *Arabidopsis* roots expressing the Glc/Gal sensor FLII[12]Pglu-700μδ6 (K_d for Glc 660 ± 160 μM) (Takanaga et al., 2008). Roots were perfused with sugar-free hydroponic growth medium and subjected to square pulses of 10 mM Glc or Gal (Figures 3A and 3B; see Supplemental Movie 1 online). Glc addition resulted in a rapid increase in cytosolic Glc levels as evidenced by a FRET index change. Exchange to sugar-free medium returned the FRET index baseline to zero with a lag time of ∼1 min. The time required to exchange the complete medium within the channel depended on the flow pressure. At the flow pressures of 2, 4, 6, and 8 p.s.i., a complete exchange of medium in the root channel was achieved in 38, 20, 13, and 9 s, respectively. The presence of roots within the observation chamber affected the filling time only slightly. For Glc/Gal perfusion experiments, a flow pressure of 6 p.s.i. was used. Consecutive Glc pulses led to reproducible FRET index changes, thereby demonstrating the robustness of the RootChip.

To test whether the chip platform is also suitable for long-term experiments, we measured growth curves and fluorescence signals of *Arabidopsis* seedlings over 24 h. To prevent Z-drift of the root during growth and thereby maintain the correct focal plane over longer time periods, the height of the observation chambers equals one root diameter. Under the commonly used
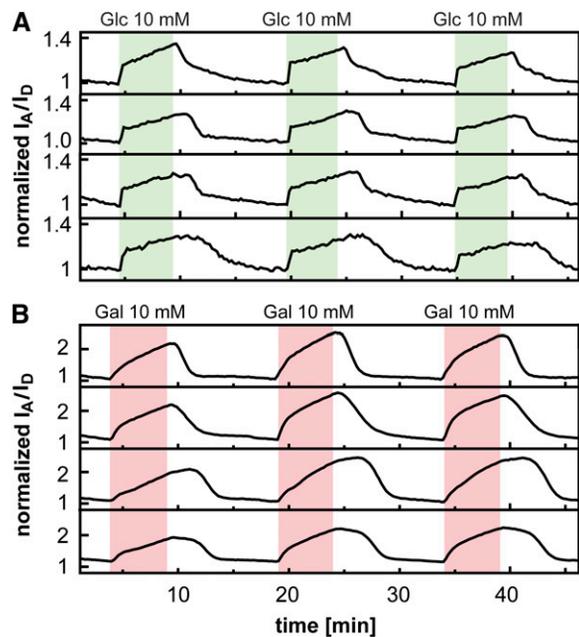

Figure 3. On-Chip Quantification of Sugar Levels Using a FRET Nanosensor.

Changes in intracellular Glc **(A)** and Gal **(B)** levels were measured with the FLII12Pglu-700μδ6 Glc nanosensor. The graphs show the normalized FRET index change (I_A/I_D) of the Glc/Gal sensor measured in the root tip. Results are shown from four representative roots. The green and red shaded bars indicate the perfusion with a square pulse of Glc and Gal, respectively.

16-h-light/8-h-dark diurnal cycle, roots of 6-d-old seedlings grew at an average rate of 2.6 ± 0.2 μm min^{-1} in the device (see Supplemental Figure 1 and Supplemental Movie 2 online), consistent with previously published data (Yazdanbakhsh et al., 2011). As expected, the growth rate declined when the experiment was performed in the dark for 24 h (Figures 4A and 4B, left panels). The simultaneously recorded FRET index indicated no significant change as root growth slowed (Figures 4C and 4D, left panels). To test for restoration of growth by exogenous sugar supply (Yazdanbakhsh et al., 2011), we perfused Glc (10 mM)

after 7 h. Glc supply stabilized root elongation at a rate of 1.1 ± 0.2 μm min^{-1} (Figures 4A and 4B, middle panels). The FRET sensor responded to Glc perfusion with an increase in the FRET index. Interestingly, the FRET index peaked during the first hour of Glc perfusion, followed by a relaxation to a new steady state level, ~15% higher compared with those observed before Glc perfusion (Figures 4C and 4D, middle panels). This higher FRET index level represents elevated intracellular Glc levels compared with those before the change of medium. The initially high increase of FRET index and subsequent relaxation indicates
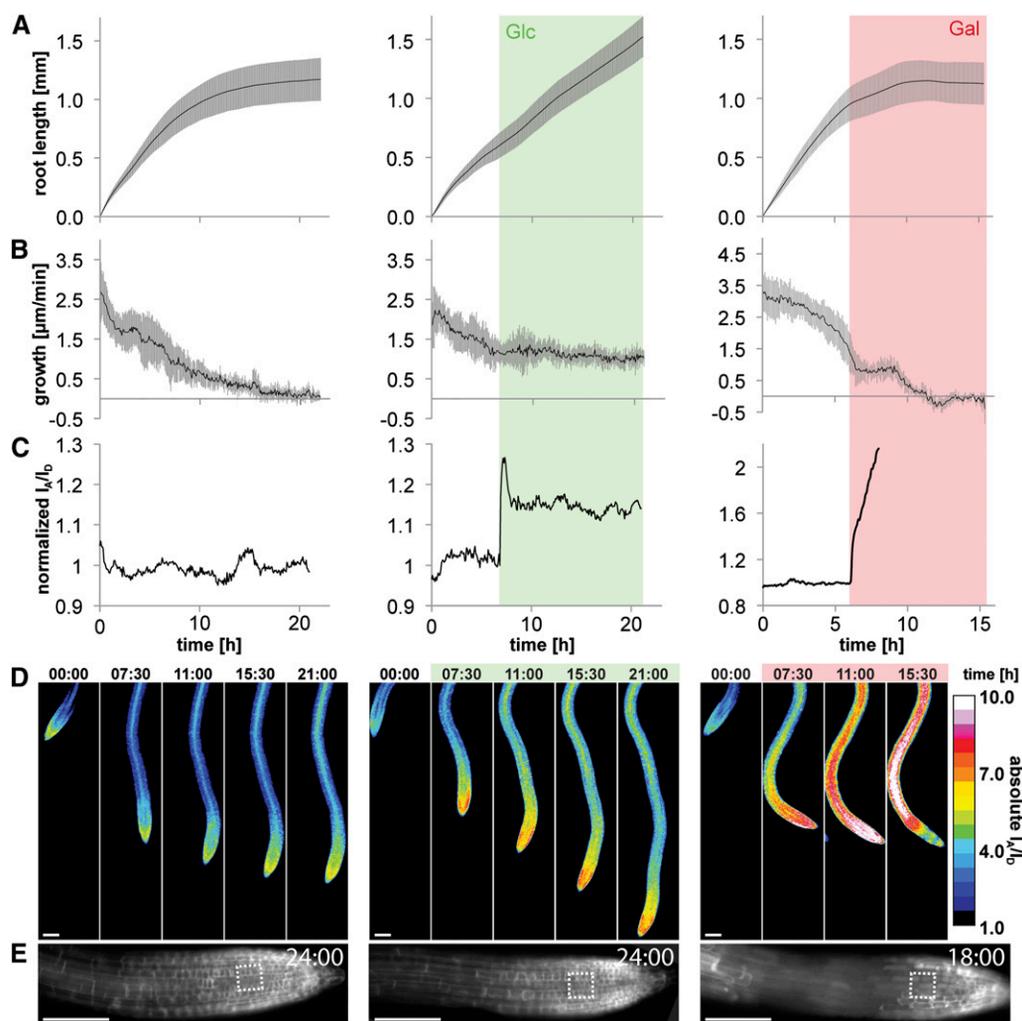

Figure 4. Long-Term Observation of Root Growth and Sugar Accumulation in The RootChip.

(A) Root length quantification under constant flow of hydroponic media without sugars in darkness (left) and with the addition of 10 mM Glc (middle) or 10 mM Gal (right). Seedlings grown in the light and were transferred to darkness at the beginning of the observation period. Green and red shaded bars indicate duration of perfusion with sugars at the 7-h time point. Quantification is derived from 12 to 15 roots grown independently on two separate chips. Gray bars represent SD.

(B) and **(C)** Corresponding growth rates and representative FRET ratio measurements of the same roots as shown in Figure 4A. The normalized FRET index change (I_A/I_D) was obtained from a 30 × 30-μm region at the root tip (dotted box in Figure 4E).

(D) False color map analysis of acceptor/donor intensity ratios in growing roots (data from Figures 4A to 4C). Green and red shaded bars indicate perfusion with sugars.

(E) Phenotypes of root tip regions after prolonged perfusion with sugar-free (left), Glc (middle), or Gal-containing medium (right; images taken at the end of the experiment [time in hh:mm]). Bars = 100 μm.

Figure 5. Live Imaging of Root Development.

Progressing root hair development in a single root grown in sugar-free medium. Time in hh:mm. Bar = 100 μm.

the induction of regulatory mechanisms to prevent uncontrolled increase of cytosolic Glc levels.

Monitoring the Effect of Gal on Root Growth

To explore the use of the chamber as a tool to monitor the effect of drugs on growth and biochemical processes, roots were exposed to Gal, which is a well-known root growth inhibitor described almost 100 years ago (Knudson, 1915). Using the same FLII12Pglu-700μδ6 sensor-expressing plants that had been used for the analysis of Glc levels, Gal accumulation was analyzed. Upon Gal perfusion, the FRET index increased in response to a 5-min pulse of 10 mM Gal and then decreased back to baseline at end of the pulse (Figure 3B). Gal accumulation and elimination rates were slower than those for Glc; however, they reached higher steady state levels, reflecting differences in transport, metabolism, and compartmentation between the two sugars. We repeated this measurement with roots of plants expressing a variant of the Glc sensor (FLIPglu-600μ) and observed a similar difference for both sugars (see Supplemental Figure 2 online). Taken together, our finding of a higher FRET index change during short perfusion pulses indicates a higher increase in intracellular Gal concentration after the pulse than for Glc.

To explore further the inhibitory effect of Gal, roots were perfused with Gal for extended periods of time. While Glc overcomes the decline in root growth observed in darkness, Gal cannot restore root growth (Figures 4A and 4B, right panels). Root growth stagnated completely after 5 h of perfusion with Gal. The corresponding FRET index showed a steep increase upon the start of perfusion, but in contrast with the previous Glc experiment, the FRET index did not relax to a new steady state. Rather, the index continued to increase to higher levels (Figures 4C and 4D, right panels). Bright-field microscopy of root tips revealed a darkening of the tissue, and epifluorescence showed loss of the normal cytosolic signal distribution, with fluorescence being evenly distributed throughout cells of the root apical meristem and elongation zone (Figure 4E, right; see Supplemental Figure 3 online). These two observations demonstrate cell death and tissue alterations after prolonged perfusion of Gal. At the same time, we observed swelling epidermal cells (see Supplemental Movies 3 and 4 online), indicating defects in cell wall integrity. Gal-induced growth inhibition and defects in cell wall structure has been reported by several authors (Ferguson and Street, 1958; Endo et al., 1968). Gal treatment results in in-

creased turgor pressure and defects in cell wall integrity (Hughes and Street, 1974; Pritchard et al., 2004), together providing a mechanism that can explain the swelling. The loss of optical transparency and increase of autofluorescence in the root cells did not allow further evaluation of the FRET index. The defects in cell wall integrity caused by the high levels of Gal accumulation described here corroborate the toxic influence of Gal on root cells and explain the growth inhibition.

Summary and Conclusions

Our data show that the RootChip can be used as an effective multichannel microfluidic platform for *Arabidopsis* root cultivation and imaging. It provides a major advance for studying root biology with the possibility of continuous imaging at cellular and subcellular resolution for several days and under conditions that allow for root growth and root hair development (Figure 5; see Supplemental Movie 5 online). The experiments presented here highlight the unique capability of The RootChip to explore root cell physiology through its ability to combine rapid control of the environment with a means to sustain robust root growth together with high-resolution live-cell imaging. In our experiments, intracellular sugar levels appeared to be altered mainly in the root tip in response to perfusion with Glc. However, various other molecules are expected or known to be taken up by other cell types, such as root hairs. The RootChip will greatly facilitate the ability to investigate nutrient uptake in different root zones, cell type–dependent metabolite flux, and the response of individual cells (such as root hair cells) to different environmental stimuli. The RootChip is generic and can be exploited for any imaging based assay. The parallel operation on this version is restricted to eight plants; minor alterations of chip design will allow growth and analysis of >30 seedlings in parallel.

METHODS

Device Fabrication

The chip was designed with AutoCAD software (Autodesk) and reproduced onto emulsion photomasks. Molds for flow and control layer were fabricated onto 4-inch silicon wafers (Stanford Microfluidic Foundry). Mold production is described in detail by Anderson et al. (2000). Briefly, the control layer features were fabricated with SU-8 photoresist and had a height of 20 mm. The flow layer was procured in a two-layer process. First, the bifurcating tree structure and inlet channel manufactured with AZ-50 XT (20-mm height). Channels were rounded following previous

published protocols. Second, the root channels were fabricated with a SU-8 photoresist (100-mm height). Molds were treated once with chlorotrimethylsilane prior to use. Chips were then manufactured individually by pouring PDMS and RTV-615 onto the silicon molds. An off-ratio protocol was used to bind the flow and control layers. The thick flow layer was formulated using a 5:1 catalyst-to-base ratio. The control layer was spin coated (30-μm thick) using a 20:1 catalyst-to-base ratio of RTV-615 to form a thin base layer. The control layer possesses all the necessary microchannels to actuate the valves on the flow layer in a push-up mechanism with a closing pressure of 15 p.s.i. (1.03 bar). The two layers were baked for 1 h at 80°C. The cast of the flow layer was then peeled off the wafer and trimmed to the correct dimensions. After soft baking, 20- (0.812 mm) and 14-gauge (1.628 mm) diameter holes were punched for the flow inlets and outlets within the flow layer PDMS piece, respectively. Additional holes for the plant holding plastic tips over the root channels were punched at a 30° angle to the device normal with a diameter of gauge 18 (1.024 mm). The flow layer is aligned onto the control layer. Chips were postbaked overnight at 80°C. Additional 20-gauge-diameter holes were punched into the finished assembled device to serve as the external control ports for the assembled device. The completed chips were plasma bonded to glass slides (0.15-mm thick) and baked for 5 min at 80°C for complete binding.

The chip carrier was designed with SolidWorks 2009 (SolidWorks) and printed on a 3D printer from uPrint with ABSplus thermoplastics. Connections were drilled in the carrier from the sides.

Root chip mask designs and fabrication protocols will be made available upon request. Additionally, the Stanford Microfluidics Foundry (http://www.stanford.edu/group/foundry/) will supply fabricated chips at cost to the academic community.

Plant Growth and Device Preparation

Arabidopsis thaliana seeds were stratified for 2 d at 4°C and germinated on hydroponic medium (Chaudhuri et al., 2011) solidified with 1% agar (Becton Dickinson Biosciences) within cut pipette tips, 5-mm long and 1-mm diameter, that were positioned in an upright position onto a plate with solidified medium. After 5 d of incubation in a growth chamber under 16 h light (90 μE m^{-2} s^{-1}) per day, the root tips had almost reached the lower tip outlet, and the tips were plugged into the plant inlets of the autoclaved device. The device was covered with half-strength hydroponic medium and incubated for 18 to 24 h. The device was then transferred onto a homemade rectangular chip carrier (10.9 cm × 10.9 cm × 2 cm [W/L/H]; recess for device 4.3 × 4.3 cm), fixed with adhesive tape, and connected to the pressure line. The chip carrier was covered with a transparent plastic sheet. To maintain the humidity within the closed chamber, the inner sides of the chip holder have surrounding water reservoirs. Upon transfer to the microscope, the device was illuminated by a ring light (Schott, Mainz, Germany) connected to a timer switch to maintain the light/dark period. The microfluidic chip is controlled by a custom-made pressure system (for instructions, see Stanford Microfluidic Foundry). A programmed LabView (National Instruments) interface was used to for automation (see also the website of the Stanford Microfluidic Foundry, http://www.stanford.edu/group/foundry/) of perfusion programs to control the microenvironment of the roots within the root chambers.

Root Imaging and FRET Measurements

Roots that had reached the chambers were imaged on an inverted epifluorescence microscope (Leica DM IRE2), equipped with a motorized stage (Scan IM 127x83; Märzhauser Wetzlar), a Polychrome V monochromator light source (TILL Photonics), a DualView beam splitter (Photometrics), and an electron multiplying charge-coupled device camera (QuantEM:512SC; Photometrics). Objectives used were ×2.5 0.07 HCX FL PLAN, ×5 0.12 N PLAN, and ×10 0.40 HC PL APO (Leica). For simultaneous imaging of cyan and yellow fluorescent fluorophores for FRET measurements, a DualView containing a ET470/24m and ET535/30m filter setup was used. Imaging data were acquired using SlideBook 5.0 software (Intelligent Imaging Innovations). Data were taken as multi-position time series with simultaneous acquisition of FRET donor and acceptor fluorophores under donor excitation, followed by acquisition of donor and acceptor under acceptor excitation.

Image Processing, FRET, and Growth Analysis

Image processing and analysis were performed in FIJI (http://fiji.sc/). Stitching of time series was performed using the 3D stitching plug-in (Preibisch et al., 2009). To reduce movement of regions of interest due to root growth, images were registered using the StackReg plug-in (Thévenaz et al., 1998), modified by Brad Busse (Stanford University). Mean gray values of regions of interest (30 × 30 μm) within the root meristem region were calculated as follows: Background was subtracted from all measured intensities; donor (ID) and acceptor (IA) intensities under donor excitation were corrected against acceptor intensity under acceptor excitation to correct for intensity fluctuation caused by focus drift, root movement, or changing sensor protein levels (during long-term measurements). Data were normalized against the baseline, and ratios of ID/IA were calculated. Ratio baselines were corrected using a third order polynomial fit (Takanaga et al., 2008). Ratio images were created using the Ratio Plus plug-in for ImageJ (Paulo Magalhães, University of Padua, Italy). Root growth was analyzed using the image analysis toolbox from Matlab version 9 (Mathworks).

Flow Analysis

To measure the exchange time of the medium within the root observation chamber, the device was flushed sequentially with dark food coloring (1:4 in hydroponic medium; Safeway) and clear hydroponic medium at different flow pressures. Images of the observation chamber were acquired at a frame rate of 50 ms. The media exchange rate was determined by measuring the change in gray scale within the root observation chamber. The time between the start of the pulse and the time point of 95% of maximum gray scale value was used as approximation of the filling time.

Supplemental Data

The following materials are available in the online version of this article.

Supplemental Figure 1. Growth Rate over 24 h under 16-h-Light/8-h-Dark Conditions.

Supplemental Figure 2. Quantification of Sugar Accumulation Measured with the FLIPglu-600μ Glc Sensor in The RootChip.

Supplemental Figure 3. Phenotype Comparison of Roots Grown in the Absence or Presence of 10 mM Glc or 10 mM Gal.

Supplemental Movie 1. Fluoresence Signal and Ratiometric Analysis of a Growing Root Perfused with Glc and Gal.

Supplemental Movie 2. Time-Lapse Imaging of Roots Growing in Observation Chambers of the RootChip.

Supplemental Movie 3. Bright-Field Time-Lapse Imaging of Root Tip Being Exposed to Gal.

Supplemental Movie 4. Fluorescence Time-Lapse Imaging of Root Being Exposed to Gal.

Supplemental Movie 5. Observation of Root Hair Development.

Supplemental Movie Legends. Legends for Supplemental Movies 1 to 5.

AUTHOR CONTRIBUTIONS

G.G., W.-J.G., W.B.F., and M.M. designed the research. G.G., W.-J.G., R.V.S and M.M. performed the research. G.G., W.B.F., and M.M. evaluated the data. G.G., W.-J.G., D.W.E, W.B.F., S.R.Q., and M.M. wrote the article. W.B.F. and S.R.Q. organized financial support.

REFERENCES

Anderson, J.R., Chiu, D.T., Jackman, R.J., Cherniavskaya, O., McDonald, J.C., Wu, H., Whitesides, S.H., and Whitesides, G.M. (2000). Fabrication of topologically complex three-dimensional microfluidic systems in PDMS by rapid prototyping. Anal. Chem. **72:** 3158–3164.

Bassel, G.W., Fung, P., Chow, T.F., Foong, J.A., Provart, N.J., and Cutler, S.R. (2008). Elucidating the germination transcriptional program using small molecules. Plant Physiol. **147:** 143–155.

Bermejo, C., Ewald, J.C., Lanquar, V., Jones, A.M., and Frommer, W.B. (2011). *In vivo* biochemistry: Quantifying ion and metabolite levels in individual cells or cultures of yeast. Biochem. J. **438:** 1–10.

Chaudhuri, B., Hörmann, F., and Frommer, W.B. (2011). Dynamic imaging of glucose flux impedance using FRET sensors in wild-type Arabidopsis plants. J. Exp. Bot. **62:** 2411–2417.

Chung, K., Kim, Y., Kanodia, J.S., Gong, E., Shvartsman, S.Y., and Lu, H. (2011). A microfluidic array for large-scale ordering and orientation of embryos. Nat. Methods **8:** 171–176.

Clark, R.T., MacCurdy, R.B., Jung, J.K., Shaff, J.E., McCouch, S.R., Aneshansley, D.J., and Kochian, L.V. (2011). Three-dimensional root phenotyping with a novel imaging and software platform. Plant Physiol. **156:** 455–465.

Endo, R.M., Thomson, W.W., and Krausman, E.M. (1968). Effects of D-galactose on the ultrastructure of bentgrass root apices. Can. J. Bot. **46:** 391–395.

Ferguson, J., and Street, H. (1958). The carbohydrate nutrition of tomato roots. Ann. Bot. (Lond.) **22:** 525–538.

Gilleland, C.L., Rohde, C.B., Zeng, F., and Yanik, M.F. (2010). Microfluidic immobilization of physiologically active *Caenorhabditis elegans*. Nat. Protoc. **5:** 1888–1902.

Hughes, R., and Street, H. (1974). Galactose as an inhibitor of expansion of root cells. Ann. Bot. (Lond.) **38:** 555–564.

Knudson, L. (1915). Toxicity of galactose for certain of the higher plants. Ann. Mo. Bot. Gard. **2:** 659–666.

Lucchetta, E.M., Lee, J.H., Fu, L.A., Patel, N.H., and Ismagilov, R.F. (2005). Dynamics of Drosophila embryonic patterning network perturbed in space and time using microfluidics. Nature **434:** 1134–1138.

Meier, M., Lucchetta, E.M., and Ismagilov, R.F. (2010). Chemical stimulation of the *Arabidopsis thaliana* root using multi-laminar flow on a microfluidic chip. Lab Chip **10:** 2147–2153.

Okamoto, T., Tsurumi, S., Shibasaki, K., Obana, Y., Takaji, H., Oono, Y., and Rahman, A. (2008). Genetic dissection of hormonal responses in the roots of Arabidopsis grown under continuous mechanical impedance. Plant Physiol. **146:** 1651–1662.

Okumoto, S. (2010). Imaging approach for monitoring cellular metabolites and ions using genetically encoded biosensors. Curr. Opin. Biotechnol. **21:** 45–54.

Preibisch, S., Saalfeld, S., and Tomancak, P. (2009). Globally optimal stitching of tiled 3D microscopic image acquisitions. Bioinformatics **25:** 1463–1465.

Pritchard, J., Tomos, A.D., Farrar, J.F., Minchin, P.E.H., Gould, N., Paul, M.J., MacRae, E.A., Ferrieri, R.A., Gray, D.W., and Thorpe, M.R. (2004). Turgor, solute import and growth in maize roots treated with galactose. Funct. Plant Biol. **31:** 1095–1103.

Samara, C., Rohde, C.B., Gilleland, C.L., Norton, S., Haggarty, S.J., and Yanik, M.F. (2010). Large-scale *in vivo* femtosecond laser neurosurgery screen reveals small-molecule enhancer of regeneration. Proc. Natl. Acad. Sci. USA **107:** 18342–18347.

Takanaga, H., Chaudhuri, B., and Frommer, W.B. (2008). GLUT1 and GLUT9 as major contributors to glucose influx in HepG2 cells identified by a high sensitivity intramolecular FRET glucose sensor. Biochim. Biophys. Acta **1778:** 1091–1099.

Thévenaz, P., Ruttimann, U.E., and Unser, M. (1998). A pyramid approach to subpixel registration based on intensity. IEEE Trans. Image Process. **7:** 27–41.

Unger, M.A., Chou, H.P., Thorsen, T., Scherer, A., and Quake, S.R. (2000). Monolithic microfabricated valves and pumps by multilayer soft lithography. Science **288:** 113–116.

Whitesides, G.M. (2006). The origins and the future of microfluidics. Nature **442:** 368–373.

Yazdanbakhsh, N., Sulpice, R., Graf, A., Stitt, M., and Fisahn, J. (2011). Circadian control of root elongation and C partitioning in *Arabidopsis thaliana*. Plant Cell Environ. **34:** 877–894.

This information is current as of March 25, 2019

Supplemental Data	/content/suppl/2011/12/16/tpc.111.092577.DC1.html
References	This article cites 23 articles, 6 of which can be accessed free at: /content/23/12/4234.full.html#ref-list-1
Permissions	https://www.copyright.com/ccc/openurl.do?sid=pd_hw1532298X&issn=1532298X&WT.mc_id=pd_hw1532298X
eTOCs	Sign up for eTOCs at: http://www.plantcell.org/cgi/alerts/ctmain
CiteTrack Alerts	Sign up for CiteTrack Alerts at: http://www.plantcell.org/cgi/alerts/ctmain
Subscription Information	Subscription Information for *The Plant Cell* and *Plant Physiology* is available at: http://www.aspb.org/publications/subscriptions.cfm